Polymer Chemistry

Effects of Linear and Branched Side Chains on the Redox and Optoelectronic Properties of 3,4-Dialkoxythiophene Polymers

Journal:	*Polymer Chemistry*
Manuscript ID	PY-ART-11-2019-001720.R1
Article Type:	Paper
Date Submitted by the Author:	28-Jan-2020
Complete List of Authors:	Reynolds, John; Georgia Institute of Technology, Chemistryand Biochemistry, Materials Science and Engineering Ochieng, Melony; Georgia Institute of Technology, Chemistryand Biochemistry Ponder, James; Georgia Institute of Technology

Effects of Linear and Branched Side Chains on the Redox and Optoelectronic Properties of 3,4-Dialkoxythiophene Polymers

Melony A. Ochieng,[a] *James F. Ponder Jr.,*[ab] *John R. Reynolds* *[ac]

[a] School of Chemistry and Biochemistry, Center for Organic Photonics and Electronics, Georgia Tech Polymer Network, Georgia Institute of Technology, Atlanta, Georgia, 30332-0400, USA

[b] Department of Chemistry and Centre for Plastic Electronics, Imperial College London, SW7 2AZ, London, United Kingdom

[c] School of Materials Science and Engineering, Georgia Institute of Technology, Atlanta, Georgia, 30332-0400, USA. E-mail: reynolds@chemistry.gatech.edu

Keywords: Dioxythiophenes, Conjugated Polymers**,** Electrochromism

Abstract

Identification of relevant structure-property relationships on solution-processable conjugated polymers have been shown to improve the performance of various redox active devices. While most research efforts have focused on the conjugated backbone, less focus has been given to the relative impact of side chain structure. Here, we report a side chain variation study tuning the optoelectronic properties on a series of 3,4-dioxythiophene-based polymers with a common conjugated backbone and differing alkyl side chains. Using a range of analysis methods, it was determined that changing from linear to branched alkyl side chains affects ionization potential,

optical bandgap, perceived color, electrochromic contrast, switching speed, and switching stability. Specifically, the polymers with branched side chains have higher onsets of oxidation and optical bandgaps, and demonstrate sudden coloration change compared to polymers bearing linear side chains. This work provides a foundation for establishing structure-property relationships on the effects of alkyl side chains on the next generation of electrochromic conjugated polymers.

Introduction

Conjugated polymers have developed rapidly due to their promising applications in low-cost, lightweight, and flexible electronics, such as organic field-effect transistors (OFETs),[1,2] light-emitting diodes (OLEDs),[3,4] organic photovoltaics (OPVs), [5,6] and electrochromic devices (ECDs).[7-9] Numerous sysyems have beem developed and the performance of conjugated polymers has steadily improved and commercial applications are seemingly imminent. This is especially true in the field of organic photovoltaics, where power conversion efficiencies exceeding 15% have been achieved,[10,11] in part due to an improved understanding of how polymer backbones and side chains can be engineered for better device performance.[12,13] In parallel, solution-processable dioxythiophene (XDOT) based polymers have been extensively researched for ECDs[14,15] due to their wide color range (optical band gap), low oxidation potentials, and high optical contrast between their vibrantly colored charge neutral states and their transmissive oxidized states.[16,17] Through backbone engineering, a series of polymers representing the complete color palette with fast switching times, low switching voltage, and long-term switching stability have been achieved.[16,18-24] However, beyond processing considerations, the effects of side chains on the properties of electrochromic polymers has only been been minimally investigated. [25-28]

An early attempt to understand the influence of side chains on the optoelectronic properties of XDOT polymers was performed in 1998.[29] This study focused on alkyl-substituted and unsubstituted poly(3,4-alklenedioxythiophene)s, where the size of the alkylenedioxy ring or the side chains were varied. It was shown that increasing the ring size, or the size of the side chains, influenced the electrochromic contrast and the electrochromic switching time. However, it was difficult to differentiate which effects could be attributed to the size of the bridging ring, and which were purely the result of side chain differences. In 2004, four new ProDOT-based polymers, synthesized by Grignard metathesis, were reported.[30] In this study, the size of the alkylenedioxy ring was consistent across all polymers, while the side chains were either linear or branched. The polymer films were able to switch reversibly from purple/magenta charge neutral state to a transmissive sky-blue state upon oxidation with sub-second switching times and electrochromic contrasts at the absorption maximum (λ_{max}) ranging from 40-70%. The study revealed that polymers in this system with branched side chains had faster switching times when compared to the polymers with linear side chains. In 2011, a similar study was conducted by the Sotzing group[31] who reported four polymers with the same 3,4-propylenedioxy ring, but varied side chain structures. The polymers with *tert*-butyl, hexyl, isopropyl, and methyl groups as the side chains distorted the backbone planarity to varying degrees, resulting in polymers films with colors ranging from yellow to purple.

The first study to focus on side chains effects in acyclic dioxythiophenes (AcDOTs) was reported in 2010.[32] The homopolymer of 3,4-bis(2-ethylhexyloxy)-thiophene, P(BAcDOT), and a random copolymer of 3,4-bis(2-ethylhexyloxy)-thiophene and 3,4-dimethoxythiophene (DMT), P(BAcDOT-DMT), were synthesized by oxidative polymerization. The branched alkoxy side chains on the P(BAcDOT) were reported to distort the backbone planarity, resulting in an orange

colored neutral polymer with an optical band gap of 2.04 eV and a λ_{max} at 483 nm. On the other hand, the random incorporation of DMT units into the backbone relaxed the steric interactions, red-shifting the λ_{max} significantly to 525 nm, resulting in a red-colored polymer. A bit surprisingly, the red-colored polymer had a more rapid switching speed of 2.3 seconds (measured at 95% of the full switch, t_{95}), while the orange-colored polymer had a slower switching speed of 5.3 seconds. Regarding ProDOT-based polymers, larger substituents at the 2-position of the propylene bridge have been shown to enhance electrochromic contrast by minimizing charge carrier (polaron and bipolaron) band tailing into the visible region from the NIR and improves switching speeds by promoting more effective counter ion diffusion through the film.[30,33] With this logic, the orange polymer was expected to have a faster switching time and higher electrochromic contrast. It is conundrums such as this that we set out to address in the present study.

To further our understanding of how side chains affect the redox and electronic properties in polymeric XDOTs, a series of AcDOT homopolymers and copolymers with linear and/or branched side chains were designed and synthesized. Within this family, three of the materials were designed to have i) an AcDOT conjugated backbone, ii) the same number of carbon atoms (eight) in the alkoxy side chains, and iii) different ratios of linear and branched side chains. To gain insight into the effect of the side chain steric interactions on the redox and associated optoelectronic properties, the linear and branched AcDOT monomers were copolymerized with 3,3-dimethyl-3,4-dihydro-2H-thieno[3,4-b][1,4]dioxepine (DMP). DMP was chosen because polymers based on this repeat unit have shown an especially high color contrast, long term redox cyclability, and the possibility of a coplanar backbone as seen in the dimer BiDMP.[27,34,35]

As illustrated in Scheme 1, it was hypothesized that: (i) branched side chains would induce torsional strain between aromatic rings due to the large van der Waals radii in the branching

position,[22] (ii) this strain would lead to a decrease in the effective conjugation length, giving rise to higher energy (lower wavelength) absorption transitions, and (iii) in DMP copolymers of branched AcDOT systems, steric interactions would be reduced, resulting in an increased effective conjugation length and a bathochromic shift of the optical transition. This principle has been demonstrated for discreate chromophore materials containing branched ProDOTs and AcDOT via DFT calculations, demonstrating the larger degree of backbone torsion as a result of the BAcDOT unit relative to a ProDOT.[36] In this work a linear AcDOT unit (LAcDOT) was investigated and compared to its branched counterpart.

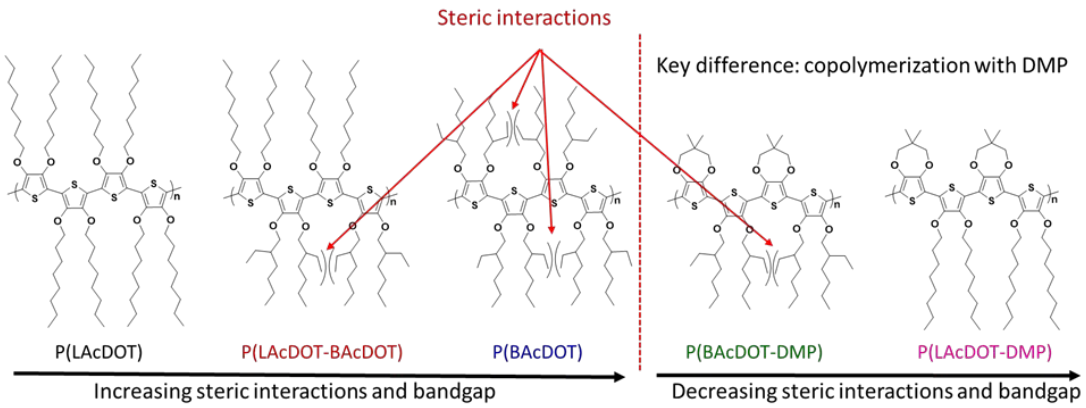

Scheme 1 Chemical structures of the XDOT polymers synthesized via either direct (hetero)arylation polymerization or oxidative polymerization, with varying steric interactions between adjacent units.

Results and Discussion

Polymerization

The monomers were synthesized through a transetherification route reacting 3,4-dimethoxythiophene with the appropriate diol in the presence of a catalytic amount of *p*-

toluenesulfonic acid (*p*-TSA), as detailed in the Supporting Information. The polymers having the repeat unit structures shown in Scheme 1, were synthesized via direct (hetero)arylation polymerization (DHAP) or oxidative polymerization; detailed synthetic routes are outlined in the Supporting Information, where the ^{1}H-NMR (Figure S1) and elemental analyses correspond to the expected repeat unit structure. The molecular weights of the polymers were estimated by gel permeation chromatography (GPC) in either tetrahydrofuran (THF) or chloroform ($CHCl_3$) (Figure S2). The results, summarized in Table 1, indicated that the polymers are of sufficient molecular weight (M_n ranging from 5 kDa to 44 kDa) where optical properties are expected to become independent of molecular weight.[37] The range in molecular weights of the polymers synthesized in this work can be attributed to differences in their solubility, as dictated by the side chain and backbone structure. The lower molecular weight of P(LAcDOT-DMP), relative to the other polymers, is due to the decreased conformational entropy of the LAcDOT and DMP units, resulting in a lower overall solubility of the copolymer and gelation in the reaction medium, thus limiting the propagation of the polymer chains. The high molecular weight of P(BAcDOT), on the other hand, is attributed to the branched side chains which allows higher molecular weight chains to form without gelation.

Table 1 Molecular weights of the polymers obtained via GPC.

Polymer	Polymerization Method	Mn (kDa) [a]	Mw (kDa) [a]	$Đ$ (M_w/M_n) [a]
P(LAcDOT)	DHAP	15	32	2.2
P(LAcDOT-BAcDOT)	DHAP	16	42	2.6
P(BAcDOT)	Oxidative	44[b]	138[b]	3.0[b]
P(BAcDOT-DMP)	DHAP	15	31	2.1
P(LAcDOT-DMP)	DHAP	5	7	1.4

[a] Values obtained from GPC in $CHCl_3$ at 40 °C calibrated *vs.* polystyrene standards. [b] Values obtained from GPC in THF at 35 °C calibrated *vs.* polystyrene standards.

Redox and Optical Properties

To investigate the electrochemical properties of the series, the polymers were dissolved in toluene at 1.0 mg/mL, except for P(LAcDOT) which was dissolved in toluene at 0.5 mg/mL. From these solutions, 4.0 μL (8 μL for P(LAcDOT)) of each solution was drop-cast on glassy carbon electrodes, allowed to dry, and electrochemically cycled between −0.5 V and 0.8 V (*vs.* Ag/Ag^+) twenty-five times to condition the films to the influx of electrolyte (referred to as electrochemical annealing, or break-in).[38] After repeated electrochemical cycling, the polymers are thought to assume their lowest energy conformation in their charge neutral states. Following the electrochemical break-in, the films were used to determine the onset of oxidation by differential pulse voltammetry (DPV), with the results presented in Table 2 and Figure S3a and b.

Table 2 Optical and electrochemical properties of the studied polymers.

Polymer	E_{ox}[a] (V *vs.* Ag/Ag^+)	λ_{max}[b] (nm)	$E_{g,\,opt}$[b]
P(LAcDOT)	0.05	513, 551, 598	1.98
P(LAcDOT-BAcDOT)	0.25	535, 583	2.01
P(BAcDOT)	0.33	466	2.13
P(BAcDOT-DMP)	0.01	545, 593	1.97
P(LAcDOT-DMP)	-0.30	560, 611	1.89

[a]Values determined by DPV as the onset of oxidation. [b]For films cast onto ITO-coated glass.
[b]Bandgap determined by the onset of light absorption from thin films.

From the results in Table 2, it is apparent that the onset of oxidation can be readily controlled by increasing the steric interaction through branched side chains. To understand the

results, first focus on the P(LAcDOT), P(LAcDOT-BAcDOT), and P(BAcDOT) series, which are expected to show progressively more steric interactions by the incorporation of a higher composition of branched side chains. In this series, the E_{ox} increases from +0.05 V to +0.25 V, then to +0.33 V. The increase in oxidation potential is primarily attributed to the steric hindrance from the branched side chains, which cause the thiophene rings to partly twist out of the plane, even in their electrochemically annealed state. This results in a greater ionization potential, thus requiring a higher voltage to oxidize the material.[21-23] The same trend is preserved when the BAcDOT and LAcDOT monomers are copolymerized with DMP, as seen in Figure S3b. P(LAcDOT-DMP) has an oxidation potential at -0.30 V, while the oxidation onset for P(BAcDOT-DMP) is +0.01 V. Looking more closely, it is apparent that the polymers with DMP have an overall lower onset of oxidation when compared to polymers comprised exclusively of AcDOT units. The difference in oxidation potential can be explained as an intricate, yet subtle, interplay of steric and electronic factors in the π-system. Broadly speaking, the DMP unit is more electron-rich, and less sterically hindered, when compared to the AcDOT unit due to the propylene bridge in the DMP, hence the overall lower onsets of oxidation in the DMP-based materials.[39-41] This trend can also be seen in the cyclic voltammograms (CVs) shown in Figure S3c and d. The P(BAcDOT) and P(LAcDOT-BAcDOT) demonstrate unusually well-defined oxidation and reduction peaks in their CVs. It is hypothesized this is due to the higher electrochemical potentials required to overcome the steric interactions induced by the branched chains. The P(LAcDOT) shows a somewhat broader and less defined CV, as is typical of conjugated polymers. Introduction of the DMP unit not only lowers the onsets of oxidation for both copolymers, but also increases the breadth of the electroactive response of the film.[27]

To allow for direct comparison of the optical switching properties between several films, measurements of optical density rather than film thickness was used.[32,42] Once the polymer was spray cast to a thickness corresponding to an approximate absorbance of ~1.0, the films were electrochemically conditioned for 25 CV cycles. After conditioning, some of the absorbance profiles were red-shifted relative to the pristine, as shown through photography in Figure 1a and Figure S4. After break-in, the normalized spectra of each film in its charge neutral state, shown in Figure 1b, were compared for more insight into the structural differences imparted by the specific side chain structure. It should be noted that, while the all AcDOT polymers show optical changes upon breaking-in, the DMP copolymers show minimal change, as seen in Figures 1a and S4. The optical band gaps follow the expected trend based on steric interactions resulting from branched side chain content. From this trend, P(BAcDOT), an orange polymer with a λ_{max} at 466 nm is the most blue-shifted. This is followed by P(LAcDOT-BAcDOT), a pink-colored polymer with 50% linear side chains and a λ_{max} at 535 nm, and P(LAcDOT), a purple-colored polymer with 100% linear side chains and a λ_{max} at 551 nm. Copolymerization of the AcDOT monomers with DMP resulted in polymers that absorb at lower energies (longer wavelength of light) than the homopolymers, which is consistent with the electrochemical results. All of the polymers studied exhibit desirable electrochromic contrast, between 54% and 73% at λ_{max}, as shown in Figure 1c and Table 3, switching from a vibrant colored state to a highly transmissive state.

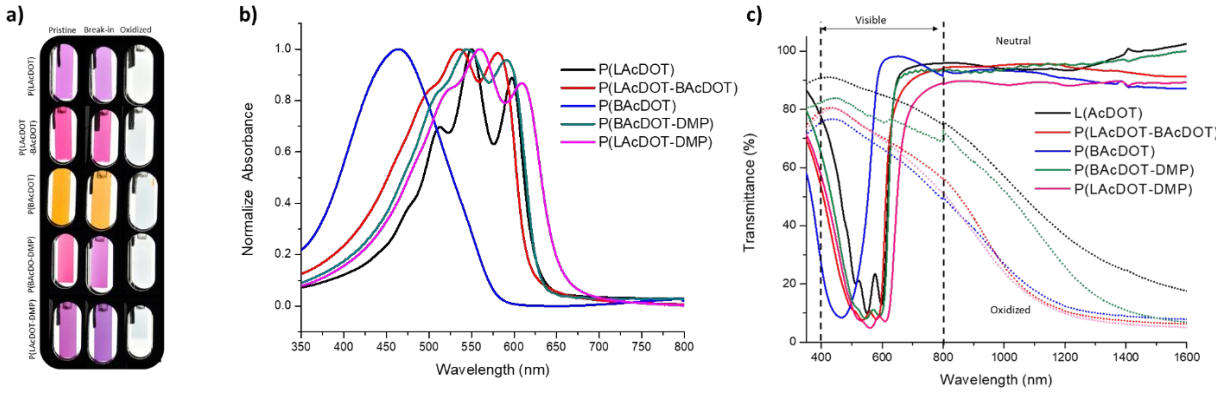

Fig. 1 a) Photographs of the polymer films in their pristine, post break-in (-0.5 V), and oxidized states (+0.8 V), all on ITO-coated glass in a three-electrode cell setup. b) Normalized absorption spectra comparing all five polymers in their charge neutral form on ITO-coated glass in 0.5 M $TBAPF_6$/PC electrolyte solution normalized to an optical density of 1.0. c) Transmittance spectra (without normalization) of the polymers in the both the charge neutral state and oxidized states.

Table 3 Electrochromic contrast, L*a*b* color coordinates for the polymers in their neutral and transmissive states, and redox switching times.

Polymer	Δ%T[a] (at λ_{max})	neutral state L*, a*, b* color coordinates[b]	oxidized state L*, a*, b* color coordinates[b]	t_{95} [b] colored to bleach (s)	t_{95} [b] bleach to colored (s)
P(LAcDOT)	73	59, 47, -30	94, -1, -3	2.4	2.5
P(LAcDOT-BAcDOT)	66	55, 63, 1	88, -3, -6	2.4	4.3
P(BAcDOT)	54	86, 34, 78	86, -4, -6	3.6	10.6
P(BAcDOT-DMP)	72	52, 53, -22	90, -2, -4	1.8	2.1
P(LAcDOT-DMP)	61	44, 40, -26	88, -4, -6	1.8	1.8

[a]Difference between steady-state transmittance at λ_{max} measured in the fully oxidized and fully neutral states. [b]Switching speeds reported correspond to the time required to reach 95% from fully colored (charge neutral) to colorless (oxidized), and fully oxidized to neutral for films cast onto ITO-coated glass.

Examining Figure 1c it is evident that all of the polymers are able to transition to NIR-

absorbing states with minimal absorption in the visible spectrum when oxidized as desired for effective electrochromic properties. It is important to note that P(BAcDOT), the polymer with the most blue-shifted absorbance spectrum, has the strongest tailing of the NIR bipolaron absorption into the visible region of the spectrum, resulting in a perceptible pale blue color in the fully oxidized state. This tailing of the bipolaron into the visible region is decreased as more linear side chains are incorporated for the all AcDOT polymers, with P(LAcDOT-BAcDOT) and P(LAcDOT) showing progressively less tailing. However, when the AcDOT monomers are copolymerized with DMP, the results do not follow the same trend. In the oxidized state, the long wavelength absorption from the more sterically hindered polymer P(BAcDOT-DMP) exhibits less tailing than P(LAcDOT-DMP). The reason for this inconsistency in the amount of tailing is currently not understood as the bipolaron peak is not directly observed, only the higher energy side of the absorbance, and tuning polaron and bipolaron absorbance profiles has not been studied.

A full spectroelectrochemical analysis was carried out on all of the polymers in order to probe the applicability of the materials as electrochromic polymers (ECPs). During the spectroelectrochemical measurement, the desired potential was applied to the film and held at that potential to reach a steady state prior to taking a spectrum, then increased in 0.1 V increments from -0.5 V to +1.1 V, the highest stable potential as determined by CV. Comparing the spectroelectrochemical results in Figure 2 and S5, all of the polymers with the branched side chains (Figure 2b, 2c, and S5a) exhibit a large optical change in both the visible and NIR over a narrow potential step window of ~0.1 V. These sudden changes for P(LAcDOT-BAcDOT), P(BAcDOT), and P(BAcDOT-DMP) occur between +0.3 and +0.4 V, +0.4 and +0.5 V, and 0.0 and 0.1 V, respectively, indicating this effect is not due to the ease or difficulty of polymer oxidation. This "jump" in optical density differs from the polymers with linear side chains, P(LAcDOT) and

P(LAcDOT-DMP), where the oxidation proceeds more gradually as a function of potential, as seen in Figure 2a and S5b. This sudden optical change in absorbance has been observed in other polymer systems.[32, 43, 44] and may be due to a cooperative intramolecular domino effect similar to the "twistons" effect, which can be considered delocalized conformation defects.[22,32,45,46] In the neutral state, the polymer exists in a nonplanar (less conjugated) form. When a small positive potential is initially applied, the polymer chain resists planarization. However, as the applied potential is increased, localized planarization begins to occur, which has a cooperative domino effect on neighboring repeat units, resulting in a sudden change in color.[47,48]

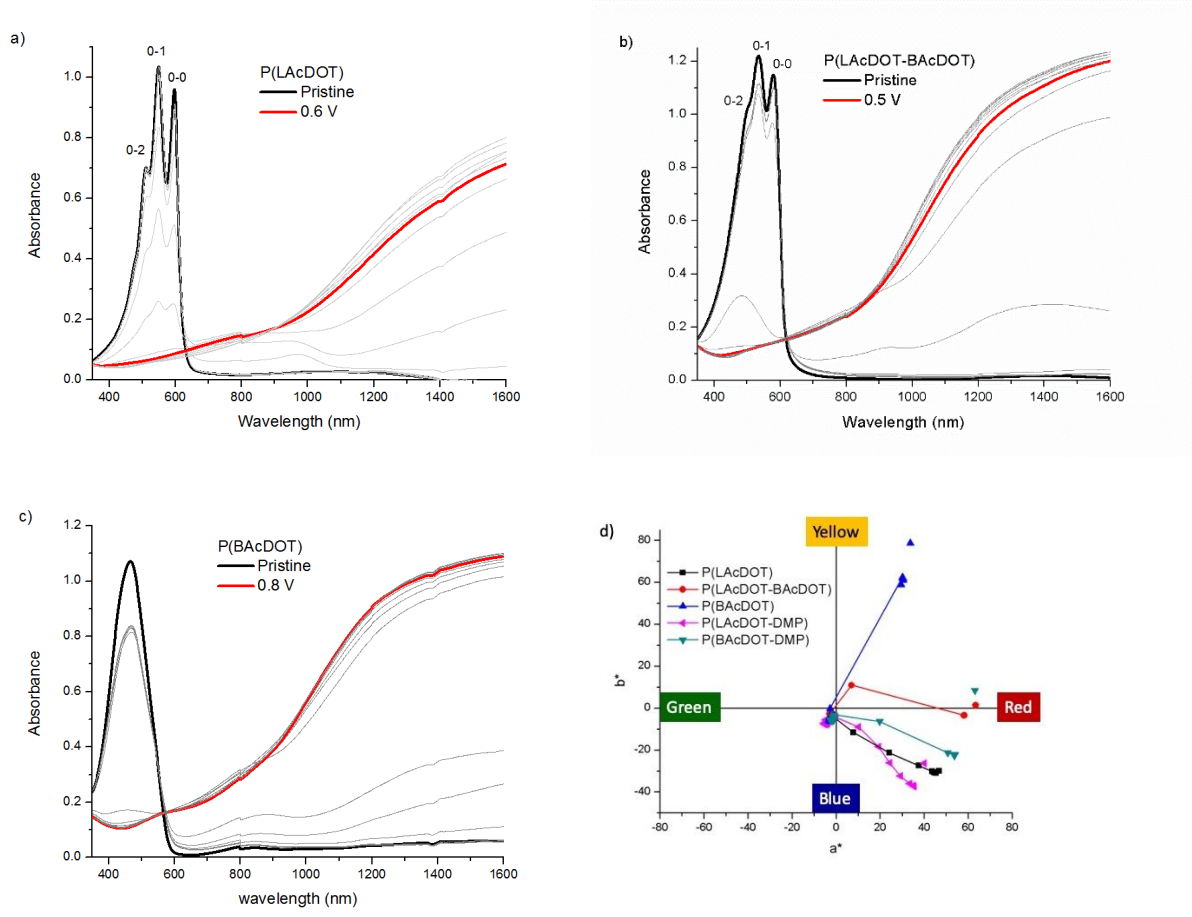

Fig. 2 Spectroelectrochemistry of a) P(LAcDOT), b) P(LAcDOT-BAcDOT), and c) P(BAcDOT),. The applied potential was increased by 100 mV steps between the fully colored (black lines) and

bleached states (red lines), with intermediate potentials shown in grey, in 0.5 M $TBAPF_6$/PC. d) Colorimetry (a*,b*) diagram of the polymers, showing the color changes occurring during electrochemical oxidation, with the separate point indicating the pristine state.

A careful comparison of the spectroelectrochemical data for the polymers reveals that steric interactions from the side chains influence the presence of aggregation features in the solid state. P(LAcDOT) has three distinct aggregation peaks at 513 nm, 551 nm, and 598 nm while P(LAcDOT-BAcDOT) has two aggregation peaks at 535 nm and 583 nm. When the branched side chain content is increased to 100% in P(BAcDOT), the resulting absorbance spectra do not show any aggregation features. The same trend is seen in P(LAcDOT-DMP) and P(BAcDOT-DMP), where P(BAcDOT-DMP) shows a decrease in aggregation as well as a decrease in the intensity of the peaks. This result supports the postulation that the presence of aggregated structures occurs in more ordered films and that steric interactions can be used to tune order/disorder in conjugated polymers. Furthermore, spectroelectrochemical data suggested preferential doping of H-aggregated species when the ratio of the 0-0, and 0-1 transitions is compared during oxidation.[49,50]

One of the most important parameters used to characterize and consider the applicability of an ECP is color, however, color is subjective to interpretation since the perception of color varies between individuals. For valid comparisons, the CIE L*a*b system was used to track the changes in color during the oxidation process. Figure 2d shows the change in the a*b* hue and saturation as the ECPs are sequentially oxidized. High values of a* and b*, initially in the as-sprayed state of the neutral polymers, is indicative of a vibrantly colored material. Upon electrochemical conditioning, the polymer chains reorganize as they dope and dedope, leading to color changes for the neutral states as shown by the second point of a* and b*. This effect is most drastic in P(BAcDOT-DMP), where the as-sprayed polymer has b* = +10 and a* = +60; after

electrochemical switching, the color coordinates change to b* = -20 and a* = +50 resulting in a color change from magenta to purple. This change is also reflected in shifts in λ_{max} and $E_{g,opt}$. After electrochemical conditioning, the potential is increased by 0.1 V and the color at each potential is recorded. Increasing the potential leads to the (a*,b*) values approaching the origin, which indicates that the polymers are becoming progressively more transmissive. Also evident in these results is the jump in the polymer's transmissivity in the cases where the material converted from the colored to transmissive form over a narrow potential range.

To determine how the side chains affect the switching kinetics in spray-cast films, the Δ%T was monitored as a function of time during the application of a square wave potential.[51] The potential square waves were executed between −0.5 V (neutral state) and +0.8 V (fully oxidized state) with various potential residence times of 60s, 30 s,10 s, 2 s, 1 s, followed by another 30 s, as shown in Figure S6a-e. The switching speeds for the polymers were reported as the time required for the polymer to reach 95% of full contrast upon bleaching and coloring during the 60 s switching period, as shown in Figure S6f. Comparing these results in Table 3, the polymers switched from colored to bleached in 1.8 s to 3.6 s, and bleached to colored in 1.8 s to 10.6 s from. With the exception of P(LAcDOT-DMP), the polymers have faster bleaching than coloration. It is hypothesized that coloration of the polymer is slower due to the injection of electrons during reduction to charge balance the polymer at the polymer electrode interface, making it insulating and slowing dedoping of the rest of the film. Taking a closer look at the switching speeds, P(LAcDOT) has the fastest coloring time of 2.5 s. Increasing the steric interaction by incorporating 50% of the branched side chains increases the coloring time to 4.3 s. When the polymer has 100% branched side chain, the coloring time is even slower at 10.6 s. The reason for this slow coloration is currently not understood, however, we hypothesize it is a result of poor electronic/ionic transport

through the P(BAcDOT) film close to the electrode as charges are being removed from the polymer chains, effectively acting as a contact resistance. Branched side chains have been shown to result in larger charge transfer resistances compared to linear side chains.[27] When the AcDOT monomers are copolymerized with DMP, the overall coloring time is faster as compared to the other three AcDOT polymers, but the material with the branched side chains still has a slower coloring time. While the structure-property relationships affecting switching speed are not fully understood, there are several consistent trends among the AcDOT and ProDOT family. Polymers containing branched AcDOTs display slow redox switching between the reduced and oxidized states, while polymers containing ProDOTs are typically faster.[23]

As stated earlier, previous studies involving AcDOTs have reported poor performance regarding redox stability, sometimes observed through film delamination upon switching.[22,32,41,44] It is unclear if this instability stems from the fact that the structure lacks a protective bridge, as in ProDOT and EDOT, or if it originates from the branched side chains. To answer this question, the long-term switching stability of P(LAcDOT) was tested. A spray-cast film of P(LAcDOT) was prepared and placed in a three-electrode cell using the same setup as the spectroelectrochemical studies. The electrolyte solution (0.5 M $TBAPF_6$/PC) was degassed *via* argon bubbling for ten minutes before the working electrode, reference electrode, and counter electrode were added. The absorption spectra of P(LAcDOT) in the neutral state was taken at -0.5 V and then at its fully transmissive state 0.8V, as shown in Figure 3 as black lines. The film was then switched between 0.5 to 0.8 V as shown in Figure S7 for 1,000 cycles with a residence time of 10 s at each applied potential. Spectra of the neutral and oxidized states were recorded again after the 1,000 cycles and are shown in Figure 3 as red lines. Extracting the ΔT % values from the chronoabsorptiometry plot shows no change in contrast. This result demonstrates that AcDOT polymers with linear side chains can have stability above 1,000

cycles, comparable to ProDOT and PheDOT systems,[44] and proves that the short switching lifetime of AcDOTs shown in the past was more likely due to the branched side polymers requiring a high oxidation potential and not due the lack of a "protective bridge".

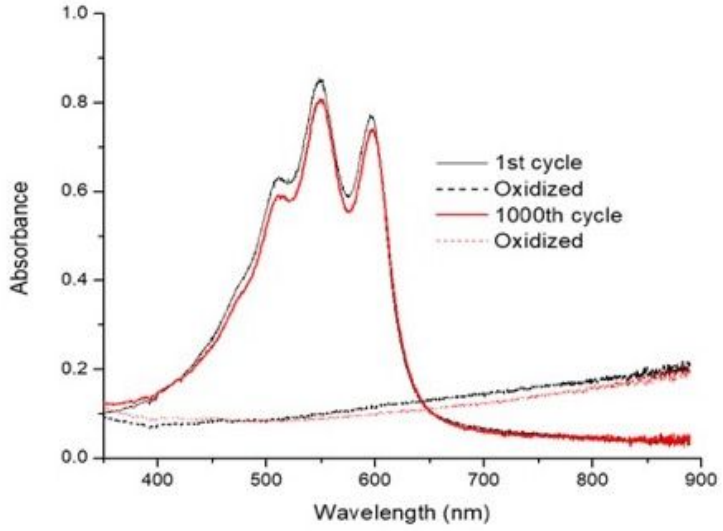

Fig. 3 Absorbance spectra of P(LAcDOT) recorded before and after 1,000 cycles in the charge neutral (-0.5 V) and oxidized state (+0.8 V) in 0.5 M $TBAPF_6$/PC.

Aggregation Effects and Thermal Properties

The optical spectra of conjugated polymers are complicated by absorbances from inter-chain aggregated and unaggregated species. Evaluating P(LAcDOT-BAcDOT) as an example in Figure S8b, the polymer is fully dissolved in dilute solution. There, the absorbance arises solely from intra-chain and non-aggregated excitations giving rise to a broad single peak. In the solid state, where the P(LAcDOT-BAcDOT) is densely packed, absorbances arise from aggregation of the polymer. This is evident by the two distinct absorption peaks and a red-shift in absorbance with respect to the solution spectra. On the other hand, the absorption profile of P(LAcDOT) shown in Figure S8a, even in a dilute

solution, is nearly identical to that observed in a solid film indicating ordered aggregates. In essence, this result indicates that linear side chains in P(LAcDOT) allows the polymer to form strong π–π stacks in solution at 25 °C, resembling the molecular geometry of the highly ordered polymer chains found in solid films. This result was surprising since most XDOT polymers have featureless absorption profiles in dilute solutions.

To answer the question of what causes the formation of ordered structures in P(LAcDOT) solutions, temperature-dependent UV-Vis measurements in toluene were performed. Even though the polymers dissolve more readily in chloroform than in toluene, toluene was chosen because it has a higher boiling point than chloroform, which allows the study of solutions over a wider temperature range. The polymer solutions were first heated to 105 °C, the temperature at which each polymer is truly molecularly dissolved. This is evident by the featureless and broad spectra shown in Figure S8, which is attributed to disordered chain conformations in non-interacting states. The polymers were then cooled to room temperature in increments of 10 °C allowing the solutions to thermally equilibrate at each temperature for ten minutes before each absorption spectrum was recorded. For P(LAcDOT) at the starting temperature of 105 °C, the spectrum has one broad peak with a λ_{max} = 510 nm. Upon cooling from 105 °C to 75 °C the broad absorption red-shifted and concurrently gained intensity (dashed lines in Figure S5a). The red shifts and increase in intensity are attributed to the planarization of the disordered chains that leads to an increase in conjugation length.[52] Decreasing the temperature to 55 °C, the absorption in the higher energy region of the spectrum decreases, while three distinct aggregation peaks appear at lower energy. These aggregation peaks have been attributed to ordered chains in an aggregated phase.[52] Below 55 °C, the absorption spectrum undergoes the most significant changes. The three distinct aggregation peaks gain intensity and red-shift; this is indicated by peaks with λ_{max} = 610 nm and λ_{max} = 540 nm with a shoulder peak at 510 nm. This red-shift in the absorption is associated

with a further planarization of the aggregated chains.[52] The P(BAcDOT) and P(LAcDOT-BAcDOT) also red-shift as the temperature is cooled to room temperature, however the polymers do not form aggregates as the feature progression is not observed, as shown in Figures S8b and c. Both DMP containing polymers show aggregation features between 560 and 580 nm, as seen in Figures S8d and e, albeit less pronounced than those seen in P(LAcDOT) and these aggregates are fully broken up by ~75 °C.

The distinct difference between P(LAcDOT) and the other polymers observed in the temperature-dependent UV-vis studies prompted us to carry out the thermal studies on all five polymers in the solid state. Thermogravimetric analysis (TGA) was performed to determine their decomposition temperatures, and differential scanning calorimetry (DSC) was used to probe for thermal transitions. TGA was carried out using a heating rate of 10 °C/min from 50 °C to 600 °C while maintaining the chamber under nitrogen. All of the polymers exhibited a high degree of thermal stability to 250 °C with a 5% weight loss in the range of 300 °C to 325 °C, as shown in Figure S9. DSC was measured three through three temperature cycles at a rate of 10 °C/min from -50 °C to temperatures below their decomposition. The first cycle was used to erase the thermal history and remove inconsistencies in the results, while the second and third cycles were used to establish reproducibly and stability. As evident in Figure 4, the third cycle thermograms for P(LAcDOT) show a distinct melting peak temperature at 169 °C and a crystallization peak temperature at 149 °C, while the thermograms of the other polymers are featureless. These peaks are a further indication of the strong intermolecular ordering of P(LAcDOT).

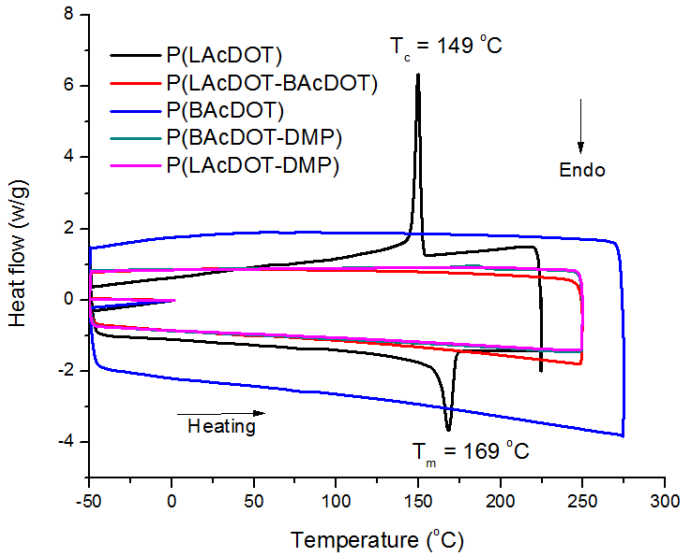

Fig. 4 The third cycle DSC thermogram for five polymers reported in this dissertation in Chapter 3 performed at 10 °C/min.

Conclusion and Discussion

Understanding the effects of side chains of electrochromic polymers is critical to the development of high-performance devices. Prior to this work, the structural impact of acyclic dioxythiophenes has only been marginally studied in terms of electrochromism, especially when compared to their more popular counterpart ProDOT-based counterparts. Here, it is demonstrated that varying side chain structure significantly affected solubility, the onset of oxidation, perceived color, switching speed, electrochromic contrast, and long-term switching stability. Furthermore, varying the side chains from linear to branched decreased interchain interactions in the conjugated polymers and reduced their propensity for aggregation in solution, as shown by temperature dependent UV-vis spectroscopy, which extended to DSC observable crystallinity in P(LAcDOT).

This property combination ultimately led to a high degree of switching stability, important to consider for possible applications in electrochromic applications. Overall, these results illustrate that side chains can and do dramatically influence the redox and optical properties of ECPs and must be considered when designing new conjugated polymer for electrochromic devices.

Acknowledgements

This manuscript is based upon research supported by the National Science Foundation through grant CHE-1506046 and the Graduate Research Fellowship Program under Grant No.DGE-1650044, along with the Air Force Office of Scientific Research (FA9550-18-1-0184). Any opinions, findings, and conclusions or recommendations expressed in this material are those of the authors and do not necessarily reflect the views of the National Science Foundation.

Conflicts of Interest

The authors declare the following competing financial interest(s): Electrochromic polymer technology developed at the Georgia Institute of Technology has been licensed to NXN Licensing. JRR serves as a consultant to NXN Licensing.

References

1. A. Tsumura, H. Koezuka and T. Ando, *Appl. Phys. Lett.*, 1986, **49**, 1210-1212.
2. H. Sirringhaus, *Adv. Mater.*, 2014, **26**, 1319-1335.
3. C. W. Tang and S. A. VanSlyke, *Appl. Phys. Lett.*, 1987, **51**, 913-915.
4. P. Kordt, J. J. M. van der Holst, M. Al Helwi, W. Kowalsky, F. May, A. Badinski, C. Lennartz and D. Andrienko, *Adv. Func. Mater.*, 2015, **25**, 1955-1971.

5. H. Kang, W. Lee, J. Oh, T. Kim, C. Lee and B. J. Kim, *Acc. Chem. Res.*, 2016, **49**, 2424-2434.

6. G. Zhang, J. Zhao, P. C. Y. Chow, K. Jiang, J. Zhang, Z. Zhu, J. Zhang, F. Huang and H. Yan, *Chem. Rev.*, 2018, **118**, 3447-3507.

7. A. L. Dyer, R. H. Bulloch, Y. Zhou, B. Kippelen, J. R. Reynolds and F. Zhang, *Adv. Mater.*, 2014, **26**, 4895-4900.

8. A. L.-S. Eh, A. W. M. Tan, X. Cheng, S. Magdassi and P. S. Lee, *Energy Technology*, 2018, **6**, 33-45.

9. A. W. Lang, A. M. Österholm and J. R. Reynolds, *Adv. Funct. Mater.*, 2019, **29**, 1903487.

10. J. Yuan, Y. Zhang, L. Zhou, G. Zhang, H.-L. Yip, T.-K. Lau, X. Lu, C. Zhu, H. Peng, P. A. Johnson, M. Leclerc, Y. Cao, J. Ulanski, Y. Li and Y. Zou, *Joule*, 2019, **3**, 1140-1151.

11. Y. Cui, H. Yao, J. Zhang, T. Zhang, Y. Wang, L. Hong, K. Xian, B. Xu, S. Zhang, J. Peng, Z. Wei, F. Gao and J. Hou, *Nat. Commun.*, 2019, **10**, 2515.

12. V. Savikhin, M. Babics, M. Neophytou, S. Liu, S. D. Oosterhout, H. Yan, X. Gu, P. M. Beaujuge and M. F. Toney, *Chem. Mater.*, 2018, **30**, 7872-7884.

13. L. Hong, H. Yao, Z. Wu, Y. Cui, T. Zhang, Y. Xu, R. Yu, Q. Liao, B. Gao, K. Xian, H. Y. Woo, Z. Ge and J. Hou, *Adv. Mater.*, 2019, **31**, 1903441.

14. Y. Wang, E. L. Runnerstrom and D. J. Milliron, *Annu. Rev. Chem. Biomol.*, 2016, **7**, 283-304.

15. X. Li, K. Perera, J. He, A. Gumyusenge and J. Mei, *J. Mater. Chem. C*, 2019, **7**, 12761-12789.

16. P. M. Beaujuge and J. R. Reynolds, *Chem. Rev.*, 2010, **110**, 268-320.

17. C. M. Amb, A. L. Dyer and J. R. Reynolds, *Chem. Mater.*, 2010, **23**, 397-415.

18. C. M. Amb, A. L. Dyer and J. R. Reynolds, *Chem. Mater.*, 2011, **23**, 397-415.

19. C. M. Amb, J. A. Kerszulis, E. J. Thompson, A. L. Dyer and J. R. Reynolds, *Polym. Chem.*, 2011, **2**, 812-814.

20. A. L. Dyer, E. J. Thompson and J. R. Reynolds, *ACS Appl. Mater. Interfaces*, 2011, **3**, 1787-1795.

21. J. A. Kerszulis, C. M. Amb, A. L. Dyer and J. R. Reynolds, *Macromolecules*, 2014, **47**, 5462-5469.

22. J. A. Kerszulis, K. E. Johnson, M. Kuepfert, D. Khoshabo, A. L. Dyer and J. R. Reynolds, *J. Mater. Chem. C*, 2015, **3**, 3211-3218.

23. K. Cao, D. E. Shen, A. M. Österholm, J. A. Kerszulis and J. R. Reynolds, *Macromolecules*, 2016, **49**, 8498-8507.

24. A. M. Österholm, D. E. Shen, D. S. Gottfried and J. R. Reynolds, *Adv. Mater. Technologies*, 2016, **1**, 1600063.

25. P. M. Beaujuge, C. M. Amb and J. R. Reynolds, *Adv. Mater.*, 2010, **22**, 5383-5387.

26. J. F. Ponder, A. M. Österholm and J. R. Reynolds, *Chem. Mater.*, 2017, **29**, 4385-4392.

27. A. M. Österholm, J. F. Ponder, M. De Keersmaecker, D. E. Shen and J. R. Reynolds, *Chem. Mater.*, 2019, **31**, 2971-2982.

28. A. Mazaheripour, E. M. Thomas, R. A. Segalman and M. L. Chabinyc, *Macromolecules*, 2019, **52**, 2203-2213.

29. A. Kumar, D. M. Welsh, M. C. Morvant, F. Piroux, K. A. Abboud and J. R. Reynolds, *Chem. Mater.*, 1998, **10**, 896-902.

30. B. D. Reeves, C. R. G. Grenier, A. A. Argun, A. Cirpan, T. D. McCarley and J. R. Reynolds, *Macromolecules*, 2004, **37**, 7559-7569.

31. T. Dey, M. A. Invernale, Y. Ding, Z. Buyukmumcu and G. A. Sotzing, *Macromolecules*, 2011, **44**, 2415-2417.

32. A. L. Dyer, M. R. Craig, J. E. Babiarz, K. Kiyak and J. R. Reynolds, *Macromolecules*, 2010, **43**, 4460-4467.

33. K. Krishnamoorthy, A. V. Ambade, M. Kanungo, A. Q. Contractor and A. Kumar, *J. Mater. Chem.*, 2001, **11**, 2909-2911.

34. D. M. Welsh, A. Kumar, E. W. Meijer and J. R. Reynolds, *Adv. Mater.*, 1999, **11**, 1379-1382.

35. L. R. Savagian, A. M. Österholm, J. F. Ponder Jr., K. J. Barth, J. Rivnay and J. R. Reynolds, *Adv. Mater.*, 2018, **30**, 1804647

36. D. T. Christiansen, D. L. Wheeler, A. L. Tomlinson and J. R. Reynolds, *Polym. Chem.*, 2018, **9**, 3055

37. H. Meier, U. Stalmach and H. Kolshorn, *Acta Polym.*, 1997, **48**, 379-384.

38. J. Heinze, B. A. Frontana-Uribe and S. Ludwigs, *Chem. Rev.*, 2010, **110**, 4724-4771.

39. L. Groenendaal, F. Jonas, D. Freitag, H. Pielartzik and J. R. Reynolds, *Adv. Mater.*, 2000, **12**, 481-494.

40. L. Groenendaal, G. Zotti, P.-H. Aubert, S. M. Waybright and J. R. Reynolds, *Adv. Mater.*, 2003, **15**, 855-879.

41. P. M. Beaujuge, S. V. Vasilyeva, D. Y. Liu, S. Ellinger, T. D. McCarley and J. R. Reynolds, *Chem. Mater.*, 2012, **24**, 255-268.

42. A. Kumar, M. T. Otley, F. A. Alamar, Y. Zhu, B. G. Arden and G. A. Sotzing, *J. Mater. Chem. C*, 2014, **2**, 2510-2516.

43. C. R. G. Grenier, S. J. George, T. J. Joncheray, E. W. Meijer and J. R. Reynolds, *JACS,* 2007, **129**, 10694-10699.

44. J. F. Ponder, B. Schmatz, J. L. Hernandez and J. R. Reynolds, *J. Mater. Chem. C*, 2018, **6**, 1064-1070.

45. M. Turbiez, P. Frère, M. Allain, C. Videlot, J. Ackermann and J. Roncali, *Chem.: Eur. J.*, 2005, **11**, 3742-3752.

46. M. Leclerc, *Adv. Mater.*, 1999, **11**, 1491-1498.

47. C. Yang, F. P. Orfino and S. Holdcroft, *Macromolecules*, 1996, **29**, 6510-6517.

48. L. Mario, *Sensors Update*, 2000, **8**, 21-38.

49. T. Eder, T. Stangl, M. Gmelch, K. Remmerssen, D. Laux, S. Höger, J. M. Lupton and J. Vogelsang, *Nat. Commun.*, 2017, **8**, 1641-1641.

50. N. J. Hestand and F. C. Spano, *Chem. Rev.*, 2018, **118**, 7069-7163.

51. S. Hassab, D. E. Shen, A. M. Österholm, M. Da Rocha, G. Song, Y. Alesanco, A. Viñuales, A. Rougier, J. R. Reynolds and J. Padilla, *Sol. Energy Mater. Sol. Cells*, 2018, **185**, 54-60.

52. F. Panzer, H. Bässler and A. Köhler, *J. Phys. Chem. Lett.*, 2017, **8**, 114-125.

TOC image

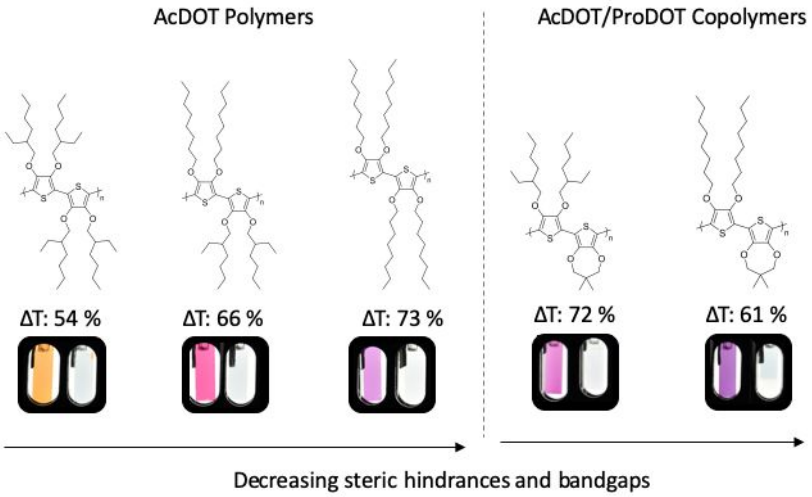
AcDOT Polymers
AcDOT/ProDOT Copolymers
ΔT: 54 %
ΔT: 66 %
ΔT: 73 %
ΔT: 72 %
ΔT: 61 %
Decreasing steric hindrances and bandgaps